Appl. Phys. B (2016) 122:26
DOI 10.1007/s00340-016-6330-2

Applied Physics B
Lasers and Optics

Photolytic-interference-free, femtosecond, two-photon laser-induced fluorescence imaging of atomic oxygen in flames

Waruna D. Kulatilaka[1,3] · Sukesh Roy[1] · Naibo Jiang[1] · James R. Gord[2]

Received: 22 October 2015 / Accepted: 5 January 2016 / Published online: 28 January 2016

Abstract Ultrashort-pulse lasers are well suited for nonlinear diagnostic techniques such as two-photon laser-induced fluorescence (TPLIF) because the signals generated scale as the laser intensity squared. Furthermore, the broad spectral bandwidths associated with nearly Fourier-transform-limited ultrashort pulses effectively contribute to efficient nonlinear excitation by coupling through a large number of in-phase photon pairs, thereby producing strong fluorescence signals. Additionally, femtosecond (fs)-duration amplified laser systems typically operate at 1–10 kHz repetition rates, enabling high-repetition-rate imaging in dynamic environments. In previous experiments, we have demonstrated utilization of fs pulses for kilohertz (kHz)-rate, interference-free imaging of atomic hydrogen (H) in flames. In the present study, we investigate the utilization of fs-duration pulses to photolytic-interference-free TPLIF imaging of atomic oxygen (O). In TPLIF of O, photodissociation of vibrationally excited carbon dioxide (CO_2) is known to be the prominent interference that produces additional O atoms in the medium. We have found that through the use of fs excitation, such interferences can be virtually eliminated in premixed laminar methane flames, which paves the way for two-dimensional imaging of O at kHz data rates. Such measurements can provide critical data for validating complex, multidimensional turbulent-combustion models as well as for investigating flame dynamics in practical combustion devices.

1 Introduction

Atomic oxygen (O) is a key intermediate species in hydrocarbon-oxidation chain-branching reactions [1, 2], pollutant formation [3], and low-temperature plasma kinetics [4]. The rates of many important reaction pathways in these systems are controlled by O because of its high reactivity [5–7]. For example, formation of thermal nitric oxide (NO), as described by the Zeldovich mechanism, is initiated by a reaction pathway where a triple bond of molecular nitrogen (N_2) is attacked by a very reactive O radical, forming NO and atomic nitrogen (N) [2]. In another example, the partial oxidation and reforming of heavy hydrocarbon fuels such as diesel and JP-8 using nonthermal plasmas in fuel cell applications encompass key reaction pathways involving O [8]. In these examples and in many other situations, accurate and nonintrusive imaging of the spatial and temporal distribution of O can be pivotal in gaining a better understanding of the reaction chemistry and dynamics, enabling validation of complex numerical models that facilitate improved hardware designs.

Laser-induced fluorescence (LIF) has been used previously in attempts to detect O in flames and plasmas because of its high sensitivity and ease of extension to 2D imaging [4, 5, 9–12]. In common with other light atomic species such as atomic hydrogen (H) and N, the lower electronic transitions accessible from the ground state of atomic O require high photon energies that correspond

✉ Sukesh Roy
sroy@woh.rr.com

✉ James R. Gord
james.gord@us.af.mil

[1] Spectral Energies, LLC, 5100 Springfield Street, Suite 301, Dayton, OH 45431, USA

[2] Air Force Research Laboratory, Aerospace Systems Directorate, Wright-Patterson AFB, OH 45433, USA

[3] Present Address: Department of Mechanical Engineering, Texas A&M University, 3123 TAMU, College Station, TX 77843, USA

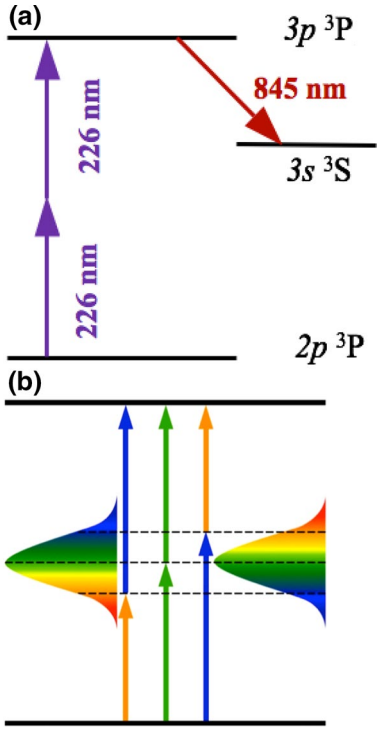

Fig. 1 **a** Two-photon excitation/detection scheme of O atoms used in this study, **b** illustration of efficient two-photon excitation of narrowband atomic transitions by broad-bandwidth, transform-limited fs pulses

to vacuum-ultraviolet (VUV) excitation wavelengths. Therefore, multiphoton excitation schemes must be used in practical diagnostic applications where the medium, in general, is opaque to VUV radiation. The commonly used excitation/detection scheme for O is 226-nm two-photon excitation of the $3p^3P \leftarrow\leftarrow 2p^3P$ transition, followed by subsequent detection of fluorescence at 845 nm from the $3p^3P \rightarrow 3s^3S$ decay. This two-photon LIF (TPLIF) scheme is shown schematically in Fig. 1a.

Multiphoton LIF schemes, in general, are plagued by relatively weak absorption cross sections and the nonlinear dependence of the fluorescence yield on laser intensity. In particular, when nanosecond (ns)-duration laser pulses are used for line or planar imaging of O, high-energy laser pulses are required to generate sufficient signal levels; hence, detected fluorescence signals are susceptible to laser-induced interferences [5–7, 13]. It has been observed in previous studies that the photolytic production of O atoms is the dominant interference mechanism, where vibrationally excited CO_2 is the primary photolytic precursor in hydrocarbon flames [7]. Other studies have also suggested that rapid photodissociation after single-photon excitation of the O_2 Schuman–Runge bands can generate significant levels of additional O in lean, premixed H_2/O_2 flames [14–16]. These interferences during the performance of quantitative TPLIF of O have prompted some research groups to implement more complicated and indirect measurement schemes. For example, Barlow et al. [3] derived O-atom number densities during the study of NO production rates in turbulent H_2/N_2 jet flames by measuring temperature, major species, OH, and NO. This scheme requires the assumption of partial equilibrium of the $OH + OH \leftrightarrow O + H_2O$ reaction, which is not necessarily valid in all H_2 flames and, in particular, when hydrocarbon fuels are involved.

In more recent studies conducted at the Combustion Research Facility at Sandia National Laboratories, picosecond (ps)-duration lasers have been investigated for TPLIF detection of O [5, 6] and H [17–20]. These studies have shown that through the use of a short-pulse laser where the peak intensity is high but the average power is low, the nonlinear excitation process in TPLIF can be enhanced, while single-photon-absorption photodissociation processes can be significantly mitigated. However, one must be mindful of the optimum pulse duration since shorter ps-duration pulses make the spectral bandwidth of the excitation laser broader than the Doppler-broadened bandwidth of the particular atomic transition, thereby reducing the spectral overlap. For transform-limited (TL) femtosecond (fs) pulses, overlapping of the laser spectral bandwidth and the Doppler-broadened atomic linewidth is unimportant because of the pairing of multiple in-phase photons for the excitation of the same transition [21, 22]. Recently, we have shown that nearly Fourier-transform-limited, fs-duration laser pulses can be significantly advantageous for two-photon excitation of H in flames [23, 24] and plasmas [25]. This process is illustrated schematically in Fig. 1b. The extreme peak intensity of fs pulses contributed favorably to the nonlinear excitation process, while significantly lower average power virtually eliminated the single-photon-absorption photolytic processes that were generating extra H in the medium. As a result of the strong fluorescence signals generated, the fs-TPLIF scheme can be readily extended to one- and two-dimensional interference-free imaging of chemical species [23, 24]. In addition, because of the inherent kilohertz (kHz) repetition rate of fs amplifiers, single-laser-shot imaging can now be performed at 1–10 kHz data rates.

In the present work, we extended the fs-TPLIF scheme to the detection of O in reacting flows. As outlined above, the oxygen atom is a key reaction intermediate in many important fundamental-combustion and plasma-related systems and applications. In particular, we explored the potential of fs-duration ultrashort laser pulses for reducing photodissociation of other species in the medium that are generating O. No significant evidence of photolytic interferences was observed in the range of $\phi = 0.7$–1.4

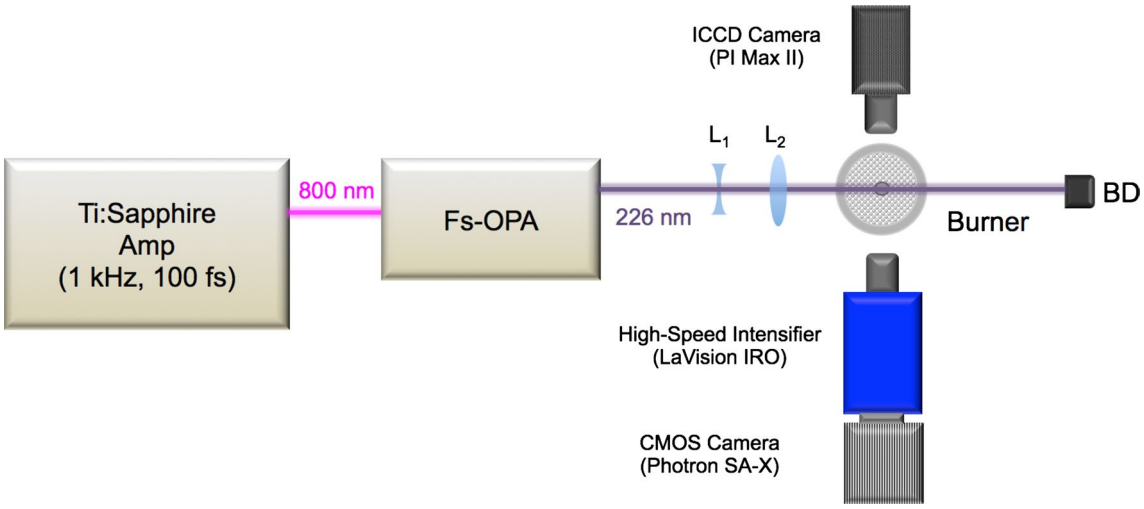

Fig. 2 Experimental apparatus

for methane (CH_4)/air flames investigated. The fs-TPLIF technique was also demonstrated in mapping the equilibrium O-atom concentration in a range of premixed CH_4/air flames stabilized in a Hencken calibration burner. The potential of fs-TPLIF for two-dimensional imaging of O at a 1-kHz data rate was demonstrated in a premixed Bunsen jet flame. The present work revealed the potential of fs-duration laser pulses for high-repetition-rate imaging of O in turbulent combustion as well as for a host of other flame and plasma applications.

2 Experimental

The experimental apparatus, as shown in Fig. 2, consists of an amplified, fs-duration, regenerative-amplifier laser system (Spectra Physics Model: Solstice) that is capable of producing nearly 100-fs [full width at half maximum, (FWHM)]-duration laser pulses at 1-kHz repetition rate, with peak pulse energies of 2.5 mJ/pulse at the fundamental wavelength of 800 nm. The output of this laser was directed to pump an optical parametric amplifier (OPA) (Coherent Model: OPerA Solo, with a UV extension module) for generating UV radiation near 226 nm to be used for the two-photon excitation scheme of O described above. Inside the OPA, the signal beam resulting from the parametric conversion process was frequency quadrupled and subsequently mixed with a portion of the fresh 800-nm input beam to generate tunable UV radiation near 226 nm. The maximum pulse energy of the UV beam at 226 nm available at the probe volume was ~7 μJ/pulse at a repetition rate of 1 kHz. The 226-nm beam was guided through several 45° dielectric laser mirrors and focused onto the probe region using a +300-mm-focal-length plano-convex lens.

Table 1 Flame conditions of premixed Bunsen flames used

Φ	CH_4 (slm)	O_2 (slm)	N_2 (slm)	CO_2 (slm)
0.81	1.87	4.59	4.98	–
1.43	1.87	3.74	4.87	–
1.43	1.87	2.61	–	1.80

A $CH_4/O_2/N_2$ Bunsen flame stabilized over a 5-mm-diameter under-expanded jet was placed at the probe volume. The flame conditions investigated are given in Table 1. The flow rates were chosen such that the height of the reaction cones for all of the flames was identical. In addition, a 12-mm × 12-mm Hencken calibration burner was also used for equilibrium number density studies. Two +50-mm-focal-length *f*/1.2 camera lenses (Nikon Nikkor AIS) were arranged in the conjugate configuration to collect the fluorescence signal and focus it back onto the detection system. A 50-mm-diameter 840-nm band-pass filter (Semrock FF01-840/12-50, 12-nm full width at half maximum, FWHM, band-pass) was mounted between the two camera lenses, which allowed >90 % transmission of the O fluorescence signal and blocked all other nearby wavelengths with an optical density (OD) >6.

Two camera systems were used for imaging the fs-TPLIF signals. For detailed study of the photolytic processes, an intensified charge-coupled-device (CCD) camera (Princeton Instruments PI Max II) was employed. This camera enabled single-laser-shot and averaged detection of the O TPLIF line images. For high-speed detection, particularly for 1-kHz imaging, a complementary metal-oxide semiconductor (CMOS) camera (Photron Model SA-X) coupled to a high-speed intensifier (LaVision Model IRO) was used. This camera/intensifier system enabled

full-frame (1024 × 1024 pixels) imaging at frame rates as high as 12 kHz. Such a high-speed imaging system is critical for utilization of the current fs-TPLIF scheme for investigation of turbulent flames where flame dynamics can be captured with sufficient spatial and temporal resolution.

3 Results and discussion

Photolytic production of O atoms by the excitation of fs laser pulses was investigated in lean, stoichiometric, and rich premixed CH_4 flames stabilized over the 5-mm-diameter under-expanded nozzle that formed Bunsen flames (Fig. 3, top panel). These premixed jet flames are ideal for investigating the photolytic production of O because of the presence of steep density gradients of O across the radial direction of the axisymmetric flame. The inner core of the flame consists of cold premixed reactants and, hence, contains no free radicals such as O atoms. The radical concentration reaches the maximum level at the flame front and decays in the outward radial direction through the products region. According to equilibrium calculations, the lean and stoichiometric flames contain up to 0.08 CO_2 by mole fraction, while the lean flame contains a mole fraction of ~0.04 excess O_2, both of which are potential photolytic precursors for producing extra O atoms. Line images of O-atom TPLIF signals were recorded at a height of 7 mm above the nozzle exits using the ICCD camera setup described above. The laser-pulse energy was varied from 0.5 to 7.0 μJ. The corresponding beam waist across the image region was estimated from the line images and found to be ~200 μm in diameter. The signal counts of shot-averaged line images were integrated in the vertical direction and are plotted as a function of the radial position in Fig. 3 for the three flame conditions investigated. Note that these radial profiles are normalized to the peak signal intensity at the location of the flame front and only the profiles from the left halves of the axisymmetric flames are shown. As these plots indicate, the relative shape of the O-atom TPLIF signal remains unchanged for each flame as the laser fluence is increased by more than an order of magnitude. Photolytic precursors are typically distributed unevenly near the flame front and in the products zone, and hence, if species-specific interfering photodissociations were present, those should be discernible by comparing the peak-normalized TPLIF profiles [5, 17–19]. Therefore, we conclude that there is no evidence of photolytic interferences in the TPLIF line profiles shown in Fig. 3. When the flame becomes fuel rich, the excess CH_4 reacts with the air entrained from the shear layer resulting in a secondary flame front, which becomes clearly visible around the radial distance of 6.5 mm in the bottom panel of Fig. 3.

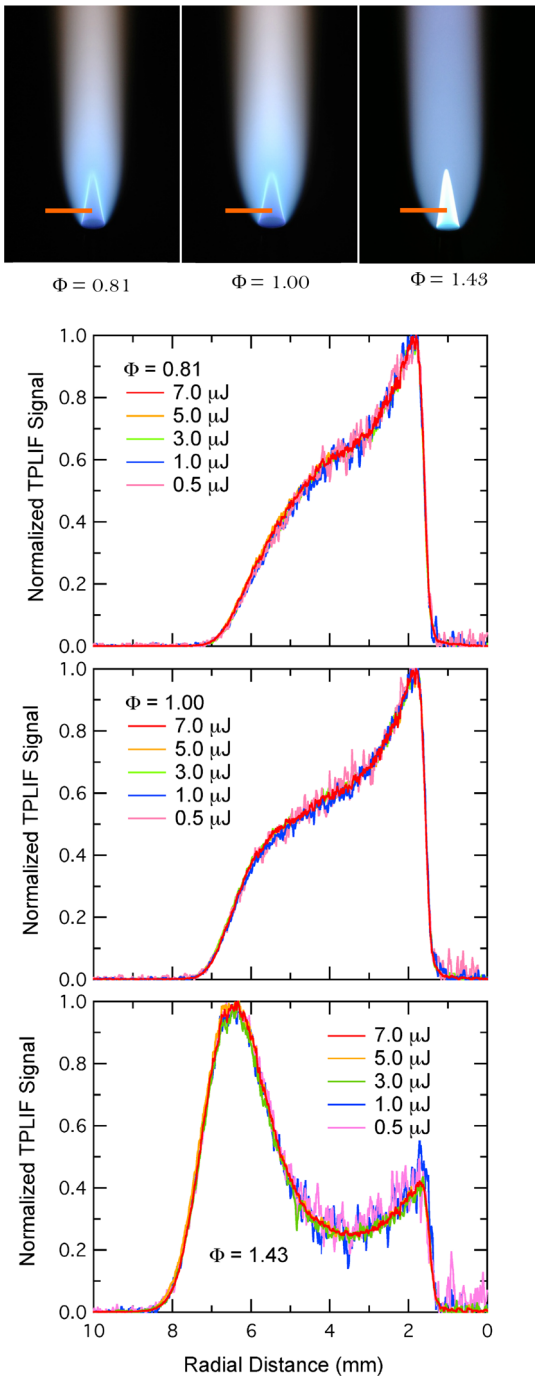

Fig. 3 Peak-normalized fs-TPLIF line profiles at varying laser-pulse energies recorded in lean, stoichiometric, and rich premixed $CH_4/O_2/N_2$ Bunsen flames (shown at *top*)

To further assess the effect of CO_2 as the main photolytic precursor for O in hydrocarbon flames, as suggested by Frank et al. [4], the N_2 dilution of the $\Phi = 1.43$ flame was completely replaced by CO_2. In this case, the inlet flow had ~28 % CO_2 by mass, and the corresponding CO_2 mol fraction in the flame zone reached ~0.2, according

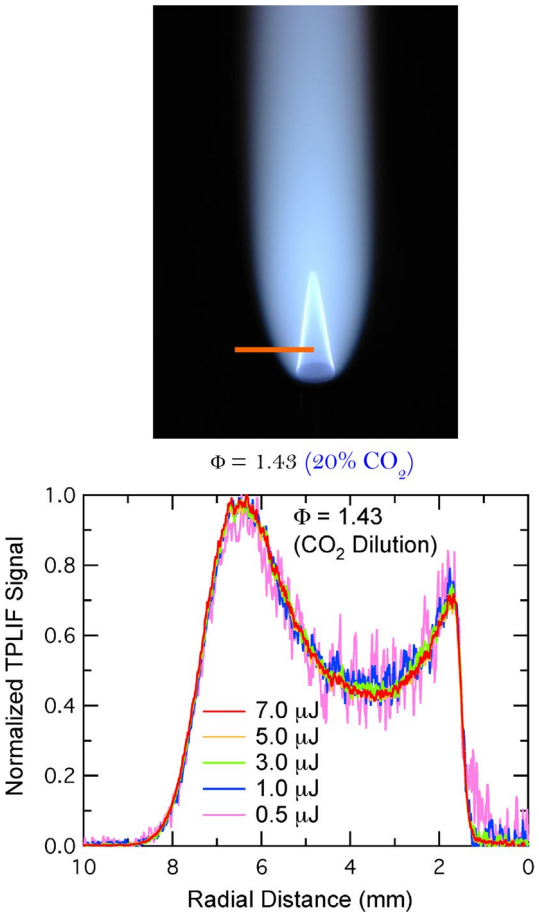

Fig. 4 Peak-normalized fs-TPLIF line profiles at varying laser-pulse energies recorded in a rich premixed $CH_4/O_2/N_2$ Bunsen flame with 20 % CO_2 dilution by mass in the inlet stream (shown at *top*)

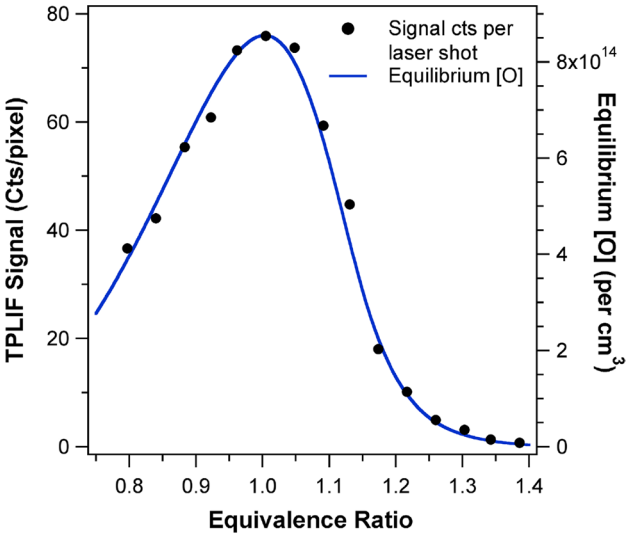

Fig. 5 Atomic oxygen fs-TPLIF signal of O as a function of flame equivalence ratio in a premixed CH_4/air flame stabilized over a Hencken calibration burner. *Solid line* represents the calculated equilibrium O-atom mole fraction

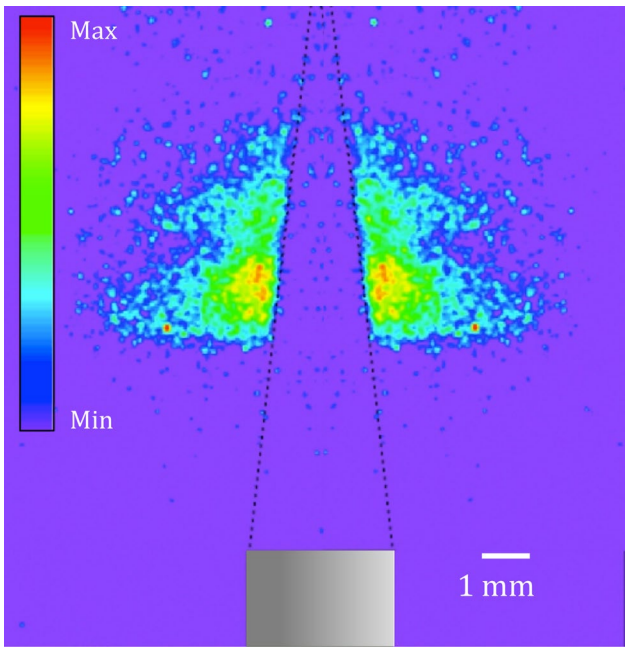

Fig. 6 Single-laser-shot fs-TPLIF image of O recorded at a pulse repetition rate of 1 kHz in a $\Phi = 1.0$ premixed $CH_4/O_2/N_2$ Bunsen flame. Height of the laser sheet is ~4 mm

to equilibrium calculations. Fs-TPLIF line images were recorded in a similar fashion while varying the UV pulse energy in the range 0.5–7.0 μJ. The resulting peak-normalized O-atom TPLIF signals are shown in Fig. 4. Similar to previous observations, the relative shape of the peak-normalized fluorescence line profile remained nearly unchanged, with only the signal-to-noise ratio improving as the laser-pulse energy was increased. Therefore, we conclude that photolytic interferences become negligible in TPLIF with the use of fs-duration laser excitation in the hydrocarbon flame conditions investigated.

The fs-TPLIF scheme was also used to measure the relative O number density in a range of CH_4/air flames that were stabilized over a Hencken calibration burner. The adiabatic flame condition achievable in this burner allows direct comparison of the measured O number density profile and the calculated equilibrium O number density. The probe volume was set ~8 mm above the burner surface. At each flame condition, 10 laser shots were accumulated in a single-image frame of the ICCD camera. The total integrated signal over the entire line image was then divided by the number of pixels in the selected region of interest and the number of laser shots to obtain the fluorescence signal counts per pixel per laser shot. The equilibrium number densities were obtained using the STANJAN chemical equilibrium code [26]. As shown in Fig. 5, very

good agreement was obtained between the measured and calculated O concentrations. No quenching correction for measured TPLIF signals was applied in these results. Typical quenching corrections for major species at equilibrium concentrations were estimated to be less that 10 % of the peak signals, which also happens to be in the same order as the experimental uncertainty of repeated single-shot fs-TPLIF measurements. Based on our previous work of fs-TPLIF measurements of H [23, 24] in similar flames, we estimate the effects of stimulated emission (SE) are also negligible.

For planar LIF imaging of O in premixed Bunsen flames, the +300-mm-focal-length spherical lens was replaced by a cylindrical lens having the same focal length to generate a laser sheet with an effective height of ~4 mm. The high-speed IRO intensifier-coupled CMOS camera system was used for kHz-rate imaging. A sample single-laser-shot fs-TPLIF image of atomic O in the $\Phi = 1.0$ $CH_4/O_2/N_2$ Bunsen flame that was recorded at a 1-kHz data acquisition rate is shown in Fig. 6. The image quality is somewhat degraded because of the limited laser energy and the nonuniformity of the spatial beam profile. The total laser-pulse energy used for the above images was ~7 μJ, corresponding to laser fluence values that are much lower than that used for the line images shown in Figs. 4 and 5. Therefore, we conclude that the single-laser-shot image shown in Fig. 6 is essentially free of photolytic interferences. The peak signal-to-noise ratio (SNR) of single-shot images shown in Fig. 6 was approximately 6:1 when the peak pulse energy of 7 μJ/pulse was used. Average shot-to-shot signal intensity fluctuations were <10 % of the peak count, evaluated from 100 consecutive single-shot images. It should be noted that the SNR could be improved significantly if more laser energy was available. However, based on current results, it is not possible to estimate the peak SNR when photolytic interferences become noticeable. By scaling the signal intensities based on line imaging results presented above, we estimate peak SNR of 100 or better is easily achievable if sufficiently higher laser energies are available.

4 Summary and conclusions

We have investigated the utilization of fs-duration laser pulses for two-photon-excited LIF detection of O in flames. The high-peak-power, low-energy ultrashort pulses significantly reduce the interfering photolytic processes during TPLIF detection. Furthermore, high-repetition-rate measurements in the range 1–10 kHz are readily achievable using titanium–sapphire-based fs amplifier systems. We have also extended the fs-TPLIF scheme for photolytic-interference-free 2D imaging of O in flames. The present results suggest that the fs-TPLIF scheme can provide significant advantages in quantitative detection and imaging of oxygen atoms in a multitude of applications ranging from fundamental flame chemistry, practical combustion devices, and numerous plasma-related reacting-flow systems.

Acknowledgments Funding for this research was provided by the United States Air Force Research Laboratory under Contract No. FA8650-15-D-2580 and by the United States Air Force Office of Scientific Research (Dr. Enrique Parra, Program Manager).

References

1. F.H. Myhr, J.F. Driscoll, Oxygen-atom concentrations measured in flames: a method to improve the accuracy of laser-induced fluorescence diagnostics. Appl. Opt. **40**, 5388–5394 (2001)
2. P. Glarborg, Hidden interactions—trace species governing combustion and emissions. Proc. Combust. Inst. **31**, 77–98 (2007)
3. R.S. Barlow, G.J. Fiechtner, J.Y. Chen, Oxygen atom concentrations and NO production rates in a turbulent H-2/N-2 jet flame. In Twenty-Sixth Symposium, ed. by A.R. Burgess, F.L. Dryer (1996), pp. 2199–2205
4. M. Uddi, N. Jiang, E. Mintusov, I.V. Adamovich, W.R. Lempert, Atomic oxygen measurements in air and air/fuel nano second-pulse discharges by two photon laser induced fluorescence. Proc. Combust. Inst. **32**, 929–936 (2009)
5. J.H. Frank, X. Chen, B.D. Patterson, T.B. Settersten, Comparison of nanosecond and picosecond excitation for two-photon laser-induced fluorescence imaging of atomic oxygen in flames. Appl. Opt. **43**, 2588–2597 (2004)
6. J.H. Frank, T.B. Settersten, Two-photon LIF imaging of atomic oxygen in flames with picosecond excitation. Proc. Combust. Inst. **30**, 1527–1534 (2005)
7. T.B. Settersten, A. Dreizler, B.D. Patterson, P.E. Schrader, R.L. Farrow, Photolytic interference affecting two-photon laser-induced fluorescence detection of atomic oxygen in hydrocarbon flames. Appl. Phys. B **76**, 479–482 (2003)
8. M.J. Gallagher Jr., Ph.D. thesis, Drexel University (2010)
9. M. Alden, H. Edner, P. Grafström, S. Svanberg, Two-photon excitation of atomic oxygen in a flame. Opt. Commun. **42**, 244–246 (1982)
10. M. Alden, H.M. Hertz, S. Svanberg, S. Wallin, Imaging laser-induced fluorescence of oxygen-atoms in a flame. Appl. Opt. **23**, 3255–3257 (1984)
11. D.J. Bamford, L.E. Jusinski, W.K. Bischel, Absolute 2-photon absorption and 3-photon ionization cross-sections for atomic oxygen. Phys. Rev. A **34**, 185–198 (1986)
12. L. Gasnot, P. Desgroux, J.F. Pauwels, L.R. Sochet, Improvement of two-photon laser induced fluorescence measurements of H- and O-atoms in premixed methane/air flames. Appl. Phys. B **65**, 639–646 (1997)
13. A.W. Miziolek, M.A. Dewilde, Multiphoton photochemical and collisional effects during oxygen-atom flame detection. Opt. Lett. **9**, 390–392 (1984)
14. J.E.M. Goldsmith, Photochemical effects in 2-photon-excited fluorescence detection of atomic oxygen in flames. Appl. Opt. **26**, 3566–3572 (1987)
15. U. Meier, J. Bittner, K. Kohse-Höinghaus, Th Just, Discussion of two-photon laser-excited fluorescence as a method for quantitative detection of oxygen atoms in flames. Symp. Int. Combust. Proc. **22**, 1887–1896 (1989)
16. D.L. van Oostendorp, H.B. Levinsky, C.E. van der Meij, R.A. Jacobs, W.T. Borghols, Avoidance of the photochemical production of oxygen-atoms in one-dimensional, 2-photon laser-induced fluorescence imaging. Appl. Opt. **32**, 4636–4640 (1993)

17. W.D. Kulatilaka, J.H. Frank, B.D. Patterson, T.B. Settersten, Analysis of 205-nm photolytic production of atomic hydrogen in methane flames. Appl. Phys. B **97**, 227–242 (2009)
18. W.D. Kulatilaka, J.H. Frank, T.B. Settersten, Interference-free two-photon LIF imaging of atomic hydrogen in flames using picosecond excitation. Proc. Combust. Inst. **32**, 955–962 (2009)
19. W.D. Kulatilaka, B.D. Patterson, J.H. Frank, T.B. Settersten, Comparison of nanosecond and picosecond excitation for interference-free two-photon laser-induced fluorescence detection of atomic hydrogen in flames. Appl. Opt. **47**, 4672–4683 (2008)
20. W.D. Kulatilaka, R.P. Lucht, S. Roy, J.R. Gord, T.B. Settersten, Detection of atomic hydrogen in flames using picosecond, two-color, two-photon-resonant six-wave-mixing spectroscopy. Appl. Opt. **46**, 3921–3927 (2007)
21. B. Broers, H.B. van den Heuvell, L.D. Noordam, Large interference effects of small chirp observed in two-photon absorption. Opt. Commun. **91**, 57–61 (1992)
22. K.A. Walowicz, I. Pastirk, V.V. Lozovoy, M. Dantus, Multiphoton intrapulse interference. 1. Control of multiphoton processes in condensed phases. J. Phys. Chem. A **106**, 9369–9373 (2002)
23. W.D. Kulatilaka, J.R. Gord, V.R. Katta, S. Roy, Photolytic-interference-free, femtosecond two-photon fluorescence imaging of atomic hydrogen. Opt. Lett. **37**, 3051–3053 (2012)
24. W.D. Kulatilaka, J.R. Gord, S. Roy, Femtosecond two-photon LIF imaging of atomic species using a frequencyquadrupled Ti:sapphire laser. Appl. Phys. B **116**, 7–13 (2014)
25. J.B. Schmidt, W.D. Kulatilaka, S. Roy, K.A. Frederickson, W.R. Lempert, J.R. Gord, Femtosecond TALIF imaging of atomic hydrogen in pulsed, non-equilibrium plasmas. AIAA Paper No. 2014-1359 (2014)
26. D. Dandy, Chemical equilibrium calculation (2015), http://navier.engr.colostate.edu/~dandy/code/code-4/